Optimal liquified natural gas (LNG) cold energy utilization in an Allam cycle power plant with carbon capture and storage

Haoshui Yu[1], Truls Gundersen[2], Emre Gençer[1*]

[1] MIT Energy Initiative, Massachusetts Institute of Technology, 77 Massachusetts Avenue, Cambridge, MA 02139, United States
[2] Department of Energy and Process Engineering, Norwegian University of Science and Technology (NTNU), Kolbjoern Hejes v. 1A, NO-7491 Trondheim, Norway
*egencer@mit.edu

Abstract: Oxy-combustion power cycles are an alternative technology for electricity generation to facilitate carbon capture and storage (CCS). Among oxy-combustion power cycles, the Allam cycle is one of the most promising technologies for power generation in terms of both efficiency and economics. Besides, the Allam cycle can also achieve a near-zero emission target at a much lower cost compared to conventional fossil fuel power plants. On the other hand, the flue gas carbon capture process and the recycled flue gas compression process in the Allam cycle consume considerable work. If the compression work can be decreased, the energy efficiency of the system can be further improved, which can enhance the competitiveness over other power generation technologies. When the fuel of the power plant is Liquified Natural Gas (LNG) instead of conventional natural gas, the LNG cold energy can be utilized to reduce the compression work of the carbon capture process and recycled flue gas compression work in the Allam cycle. In this study, we investigated different ways to utilize the LNG cold energy for both a stand-alone power plant and a combined power plant and LNG regasification cogeneration system. A superstructure incorporating many possible flowsheets is proposed in this study. A simulation-based optimization framework is adopted to optimize the superstructure. The results indicate that direct integration of LNG regasification and flue gas liquefaction performs well for the stand-alone power plant, while the organic Rankine cycle integration scheme is the best choice for the cogeneration system.

Keywords: LNG cold energy, Allam cycle, Carbon capture, Organic Rankine cycle, Process integration

1. Introduction

Since the Industrial Revolution, the atmospheric CO_2 concentration has increased from 280 ppm in 1760 to 402 ppm in 2016 [1], which accelerates the climate change. Low- or zero-carbon electricity will become the dominant form of energy in the energy supply by 2050 [2]. Carbon capture and storage (CCS) is perceived as a critical technology to alleviate climate change [3]. The power sector is responsible for 37% of the total man-made greenhouse gas (GHG) emissions globally [4]. However, reducing the CO_2 emissions in a power plant is challenging technically and economically [5]. The carbon capture technology in power plants can be categorized as pre-combustion, post-combustion and oxy-combustion carbon capture [6]. Amine scrubbing [7], membrane technology [8], adsorption [9] and absorption [10] are several examples of post-combustion carbon capture technologies. Integrated Gasification Combined Cycle (IGCC) with CO_2 separation before combustion is an example of pre-combustion carbon capture. However, there are still technical problems with hydrogen turbines to be solved for this carbon capture option. The oxy-combustion alternative uses high purity oxygen instead of air as the oxidizer so that the flue gas is composed of mainly water and CO_2 [11]. Nowadays, oxy-combustion [12] and cryogenic CO_2 separation driven by LNG cold energy [13] are drawing increasing attention from the research community. The Allam cycle, also known as NET cycle is estimated to have the lowest cost of electricity (88.3 €/MWh) compared with other cycles (in the range 93-95 €/MWh) [14] and it is the most promising technology both in terms of efficiency and economics [15]. The Allam cycle is an oxy-combustion power cycle, which facilitates the carbon capture process since the separation of CO_2 from nitrogen is not required [16]. Even though the flue gas is high purity CO_2, the flue gas has to be cooled down first and then water is condensed and removed. Finally, the flue gas is compressed to high pressure for transportation and storage. The compression work of the flue gas results in the energy penalty due to CCS implementation. As for the fuel of the power cycle, Liquified Natural Gas (LNG) is playing an increasingly important role in the energy market. LNG global trade is continuously growing and reached 293.1 million tons in 2017 [17]. LNG is transported below -160°C at atmospheric pressure and the volume is decreased by 600 times compared with the counterpart natural gas. Therefore, LNG has to be regasified to natural gas before sent to the end users, and the cold energy in the LNG can be utilized. LNG cold energy utilization in power plants has been investigated extensively in the literature. Lee and You [18] proposed a novel integrated system combining a Liquid Air Energy Storage (LAES) system, Organic Rankine Cycle (ORC) system and LNG regasification process. This integrated system can flexibly release energy due to the LAES system. Lin et al. [19] proposed a novel CO_2 transcritical power cycle to recover the waste heat from the conventional gas turbine exhaust and the LNG cold energy simultaneously. CO_2 as the working fluid of the power cycle is circulated between flue gas of the gas turbine and the LNG. Shi et al. [20] proposed to utilize the LNG cold energy for inlet air cooling and compressor inter-cooling in a conventional combined cycle power plant. Xiong et al. [21] investigated the integration of LNG regasification with an Air Separation Unit (ASU) and a CO_2 capture process. LNG cold energy can be fully utilized to reduce the energy penalty. The main barrier for the commercialization of CCS lies in the high capital cost and energy penalty [4]. Therefore, process integration and optimization of the CCS process with existing power cycles or novel power cycles can be used to reduce the capital cost or energy penalty, which can accelerate the commercial deployment of CCS. The previous studies mainly focused on the LNG cold energy utilization in a conventional combined cycle power plant. The studies focusing on the Allam cycle are quite limited. In this study, the utilization of LNG cold energy in an Allam Cycle power plant with carbon capture is investigated. Different system configurations are proposed, optimized and compared based on a simulation-based optimization framework. This study is the pioneering work to investigate the LNG cold energy utilization in an Allam cycle power plant considering carbon capture to achieve the zero-emission target.

2. Allam cycle and organic Rankine cycle (ORC) description

The Allam cycle is a low-pressure ratio Brayton cycle with high-pressure recirculating CO_2 as the working fluid [22]. The flowsheet of an Allam cycle is illustrated in Fig. 1. Oxygen from the ASU is pressurized and heated before fed into the combustor, where recycled flue gas mixes with the fuel and oxygen. The high pressure and high temperature flue gas expands through a turbine to generate electricity. After expansion, the low-pressure flue gas preheats the oxygen, high-pressure recycled flue gas to the combustor and turbine coolant in multiple heat exchangers or one multistream heat exchanger. The low-pressure flue gas is further cooled down to remove water and then split into two sub-streams. Most of the flue gas is recompressed to a dense state and then pumped in a supercritical state before being recycled to the high-pressure combustor. The residual stream is fed to the CO_2 purification and compression section, where the flue gas is compressed to higher pressure for transportation and storage. At ambient temperature, the density of CO_2 is about 700 kg/m^3 for pressures greater than 80 bar. To ensure stable operation of the CCS, the final target pressure of captured flue gas is generally recommended to be greater than 86 bar to avoid sharp changes in compressibility for the temperature range of the pipeline system [23]. In this study, the target pressure of CO_2 is set as 86 bar beyond which CO_2 can be further pressurized by pumps. The parameters and important system metrics of the Allam cycle power plant are obtained from [15] and [24] as listed in Table 1. This power plant can generate 427.7 MW electricity without considering the natural gas compression work. However, it should be noticed that the recycled flue gas compression work is 103.95 MW, which takes up to almost 16.45% of the gross power output. As shown in Fig. 1, the captured flue gas compression process (Zone 1), natural gas compression process

(Zone 2), and recycled flue gas recompression process (Zone 3) consume huge amounts of compression work, which results in an energy penalty for the power plant. In this study, we aim at integrating the LNG regasification process with the above three zones in the Allam cycle. Different system configurations to utilize LNG cold energy are proposed and compared in this study.

Table 1. Key parameters of the Allam cycle

Parameters	Value	Unit
Natural gas flowrate	59,470	kg/h
Flue gas flowrate for CCS	157,300	kg/h
Recycled flue gas flowrate	4,704,000	kg/h
Flue gas pressure	33.00	bar
Gross power output	631.95	MW
Recycled flue gas compression work	103.95	MW
ASU work consumption[1]	100.3	MW
Power output[2]	427.7	MW
Natural gas compression work	4.75	MW
Net power output	422.95	MW

[1]In reference [15], the ASU work consumption is 85.45 MW, however, the energy balance is not satisfied in that paper. The ASU work consumption should have to be 100.3 MW to get the net power output 422.95 MW. In essence, this number has no effect on this study since ASU is out of the scope of our study. [2]This refers to the power output ignoring the natural gas compression work.

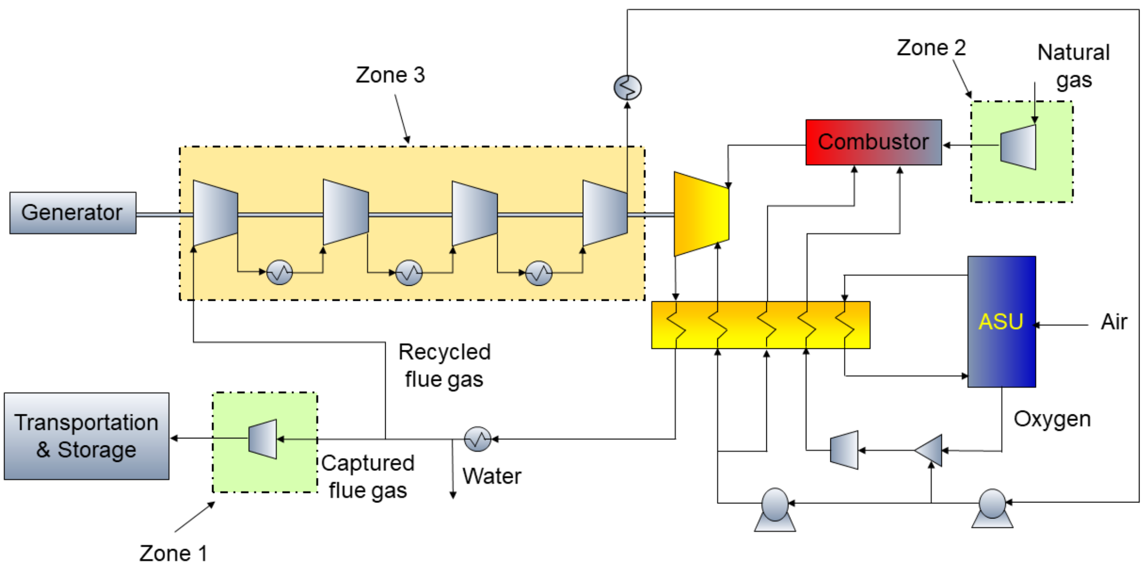

Fig.1 The flowsheet of an Allam power cycle [15]

To utilize the LNG cold energy to a larger extent, an organic Rankine cycle (ORC) between the flue gas and the LNG stream can be configured. There are two benefits of the integration of an ORC. An ORC can balance the heat loads of flue gas and LNG, additionally can also generate extra electricity. A certain amount of electricity can be generated from the ORC, while the condensation heat load of the flue gas is reduced by such amount of the electricity output from the ORC. Yu et al. [25] proposed to adopt an organic Rankine cycle to recover LNG cold energy with seawater or waste heat from the industry as the heat source. The flowsheet of a basic ORC is illustrated in Fig.2. A basic organic Rankine cycle consists of a pump, an evaporator, a condenser and a turbine [26]. In this study, the flue gas is the heat source of the evaporator and the LNG is the heat sink of the condenser. Another heat exchanger (HEX-ORC) between the flue gas and LNG is also configured to fully utilize the LNG cold energy in this study.

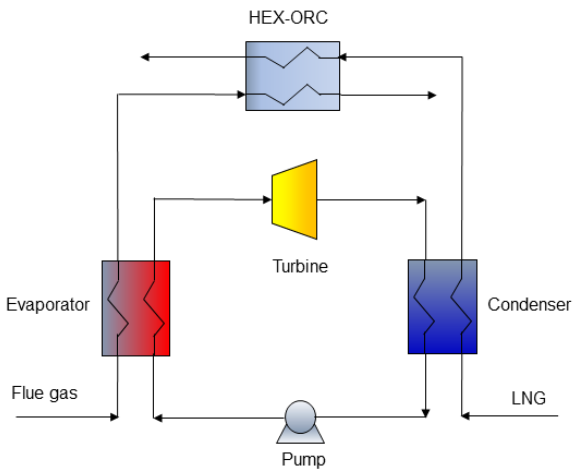

Fig.2 Flowsheet of the ORC utilizing LNG cold energy

3. Integrated system configurations

Captured flue gas, as shown in Fig.1, can either be compressed to the desired pressure by a gas compressor or be liquified by refrigeration systems and then pumped to the desired pressure for transportation and storage [27]. In the latter option, the pump work is significantly less than the compression work. In addition, a pump is generally much less expensive than a gas compressor [28]. Cold energy in LNG can be regarded as an off-the-rack refrigeration system. For the Allam cycle, as shown in Fig.1, the LNG regasification process can be integrated with the highlighted zones. However, the integration scheme depends on how much LNG is available. It should be noted that the recycled flue gas flowrate is much larger than that of the captured flue gas in the Allam cycle. If the amount of LNG is limited, only Zones 1 and 2 can be integrated with the LNG cold energy. However, when the LNG throughput is large, all zones in Fig.1 can be integrated with the LNG regasification process. Therefore, two different scenarios, namely a standalone power plant and a cogeneration system are investigated in this study. For the standalone power plant, the LNG is regasified and then totally burned as the fuel in the Allam cycle. The optimal integration between the LNG regasification process and Zones 1 and 2 with/without an ORC is investigated. For the cogeneration system, the LNG is first regasified and then most of the natural gas is directed to other end users in pipelines, while only a small part of the natural gas is burned in the Allam cycle power plant. Different system configurations are proposed for each scenario.

3.1. LNG cold energy utilization in a standalone power plant

For a standalone power plant, the LNG flowrate is the same as the required natural gas flowrate as shown in Table 1. Since the LNG flowrate is limited, the LNG regasification process is only integrated with Zones 1 and 2 as shown in Fig.1. A superstructure of the integrated system is proposed as illustrated in Fig.3. The condensed water stream and vented flue gas are omitted in the superstructure for clarity. The superstructure contains many possible flowsheets and some of the units may not exist in specific flowsheets.

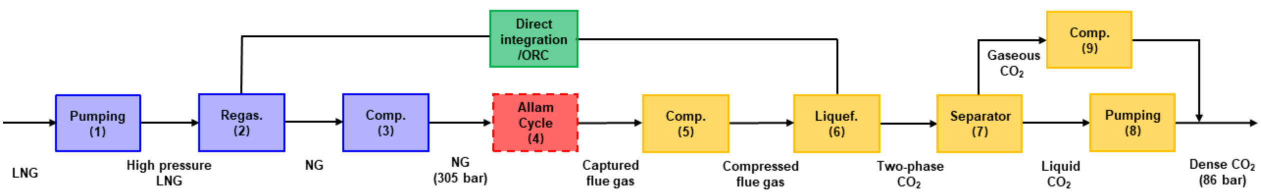

Fig.3 Superstructure of the integrated process in a standalone power plant

There are several ways to improve the efficiency of the system based on the superstructure: (1) The LNG should be pumped to higher pressure before regasification to save the compression work; (2) The LNG cold energy released during regasification should be utilized to liquefy the flue gas to save compression work for the flue gas. The LNG regasification process and flue gas liquefaction process can be integrated directly or indirectly via an ORC. However, the amount of LNG cold energy depends on the regasification pressure. The LNG cold energy released at 305 bar is not enough to completely liquefy the flue gas. To achieve total liquefaction of the flue gas, the LNG regasification pressure must be lower than a specific value. Therefore, there is a trade-off between the LNG compression work and flue gas compression work.

The objective of this work is to identify the most efficient flowsheet in the superstructure presented in Fig.2 of a standalone power plant. Whether the ORC should be integrated in the system and the corresponding operation conditions of the ORC are going to be determined simultaneously. The optimal flowsheet should balance the trade-off among the LNG regasification and pressurization process, the flue gas liquefication and pressurization process, and the ORC power generation process. Even though the optimal flowsheets are of utmost interest, special flowsheets with known boundary conditions should be analyzed to see the value of process integration and understand the optimal flowsheet better. Seven flowsheets including the optimal flowsheets embedded in the superstructure are analyzed in the following section.

Process A (Base case)

First of all, a reference case without any process integration is simulated as the baseline. In the base case, the LNG is pumped to 305 bar and then regasified by an open rack vaporizer with seawater as the heat source. The flowsheet of the base case (A) is illustrated in Fig.4. The flue gas from the Allam cycle is split into two substreams, namely captured flue gas and recycled flue gas to make a clear distinction in this study. It should be noticed that a small amount of the captured flue gas stream can be vented since the capture ratio is set as 90% in this study. The captured flue gas stream has to be compressed to dense state (86 bar) for CCS, while the recycled flue gas needs to be compressed and pumped to 305 bar and sent back to the combustor in the Allam cycle as the working fluid. Process A is an inefficient flowsheet since both process integration and LNG cold energy utilization are not considered. To take advantages of process integration and LNG cold energy, the integrated flowsheets embedded in the superstructure in Fig.3 are presented as follows.

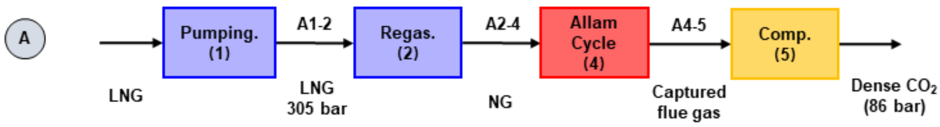

Fig.4 Flowsheet of Process A (base case)

Process B (Direct integration without flue gas compressor)

Based on Process A, new integration opportunities arise. In Process B, the assumption is that flue gas is totally liquified by the LNG. If the LNG is regasifed under 305 bar, the LNG cold energy released is not enough to totally liquify the flue gas, which will be discussed in detail in the results and discussion section. Therefore, the LNG is regasified at an intermediate pressure and then a compressor is required to meet the specification of the Allam cycle. The advantage is that no compressor is required for the flue gas since the LNG cold energy in this case can completely liquify the flue gas. The detailed integrated flowsheet is shown in Fig.5.

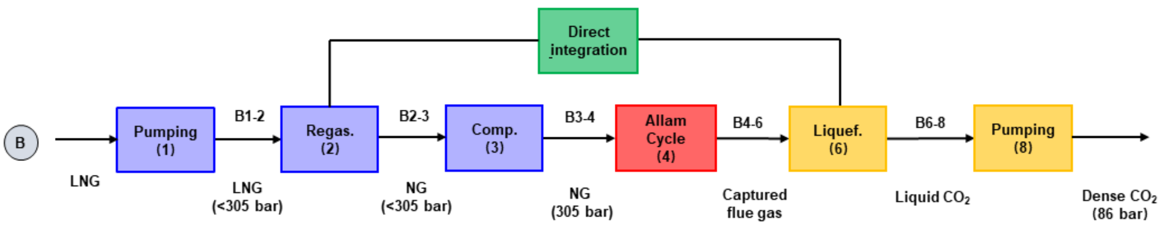

Fig.5 Flowsheet of Process B

Process C (Direct integration without natural gas compressor)

As an alternative to Process B, the natural gas can be pumped to the target pressure (305 bar) directly before regasification, and thus the compressor for the natural gas is not required. However, the LNG cold energy is not enough to completely liquify the flue gas in this case. The flue gas can be partially liquified by the LNG cold energy released at 305 bar. Therefore, a separator has to be introduced in this system. The gaseous stream has to be compressed to the target pressure by a compressor while the liquid stream is pumped to the target pressure. The flowsheet of Process C is illustrated in Fig.6.

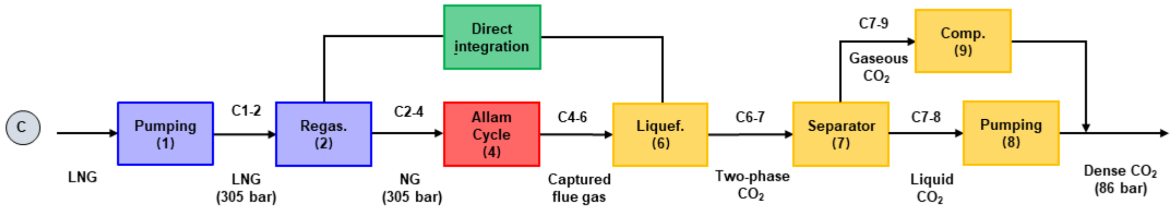

Fig.6 Flowsheet of Process C

Process D (Optimal flowsheet for direct integration)

The optimal flowsheet for direct integration should be determined to make a trade-off between the natural gas compression work and the captured flue gas compression work. Process B is prone to save the captured flue gas compression work and thus the LNG is regasified at an intermediate pressure less than 305 bar to supply enough cold energy to totally liquefy the flue gas. In Process C, the LNG is pumped to 305 bar directly to save the compression work of natural gas and a separator and compressor have to be configured in this case. A more comprehensive flowsheet, where both the natural gas compressor and flue gas compressor are incorporated as shown in Fig.7. The LNG pressure after pumping is set as a free variable. When the LNG pressure after pumping reaches the upper bound (305 bar), the compression of natural gas is no longer necessary. The optimal trade-off between natural gas compression and flue gas compression is identified automatically by an optimization algorithm. The optimization of the integrated system will be discussed in detail in Section 4.

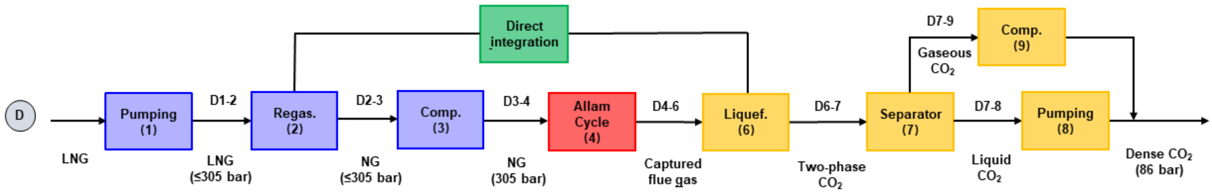

Fig.7 Flowsheet of Process D

Process E (ORC integration without flue gas compressor)

Since the LNG cold energy is not enough to completely liquify the flue gas unless the LNG regasification pressure is below a certain value. For higher LNG regasification pressures, the condensation heat of the flue gas is larger than the evaporation heat of the LNG. A more detailed energy analysis is performed in Section 5. To utilize the LNG cold energy more efficiently, an ORC is integrated in the system in Process E as shown in Fig.8. Compared with Process B, the only difference is that an ORC is configured between the flue gas liquefaction process and the LNG regasification process.

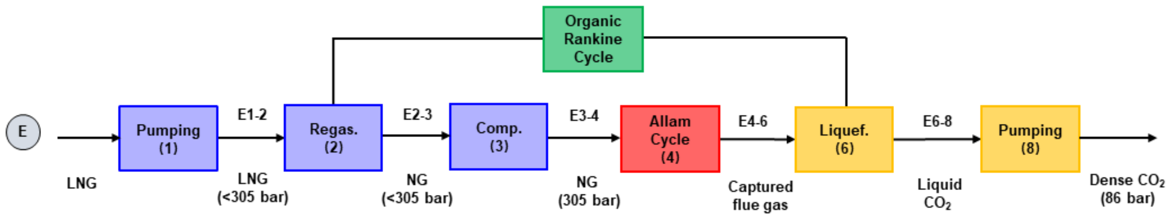

Fig.8 Flowsheet of Process E

Process F (ORC integration without flue gas compressor)

Similar to Process C, if the flue gas is totally liquified by the ORC and LNG jointly, the regasification pressure of LNG has to be less than 305 bar to release enough cold energy. To avoid compressing natural gas and thereby saving both work and the investment in a compressor, the LNG is pumped to 305 bar directly in Process F as shown in Fig.9. In this process, a separator has to be configured due to the insufficient LNG cold energy released at 305 bar.

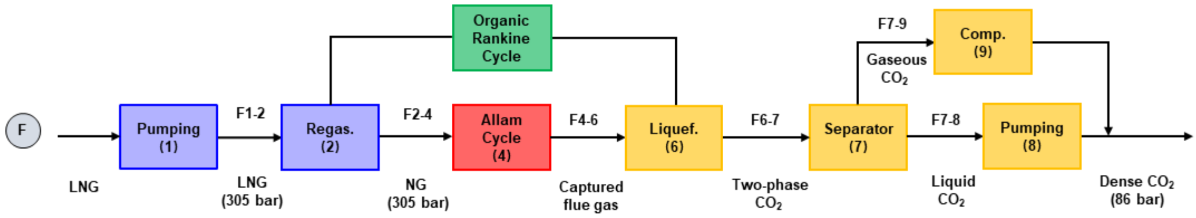

Fig.9 Flowsheet of Process F

Process G (Optimal ORC integration)

In a similar way, a comprehensive ORC integration flowsheet (Process G) incorporating both the natural gas compressor and the captured flue gas compressor embedded in the superstructure is illustrated in Fig.10. This flowsheet could be more energy efficient than any other configurations. However, this flowsheet is more complex since both the natural gas compressor and the captured flue gas compressor have to be configured in this case. Process E and F are subsets of Process G and Process G may degenerate to Process E or F depending on the optimization results.

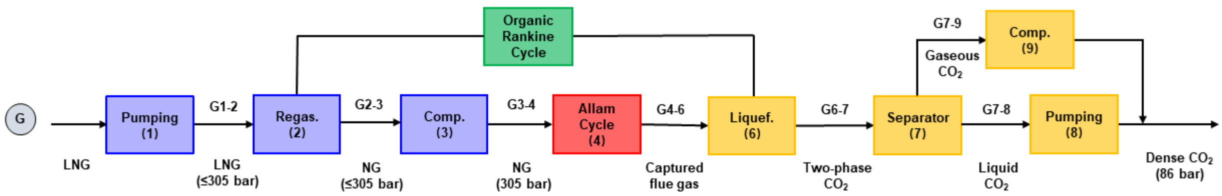

Fig.10 Flowsheet of Process G

3.2. LNG cold energy utilization in a cogeneration system

Generally, the throughput of an LNG terminal is fairly large and the regasified LNG is directed through a natural gas pipeline to various end users. In this case, the Allam cycle power plant can be integrated with the LNG regasification plant. The integrated system is termed as a cogeneration system since both electricity and natural gas are the products of the integrated system. The Incheon LNG terminal in South Korea regasifies 1620 t/h LNG using open rack evaporation technology [29]. In this study, the throughput of the LNG terminal is assumed to be 1620 t/h as well. The target pressure of the natural gas, which depends on the application, is assumed to be 30 bar. For the cogeneration system, the LNG is split into two different substreams, one stream is fed to the Allam cycle at 305 bar and the other stream is regasified and directed to the natural gas pipeline at 30 bar. Since the pressures of these two streams are totally different, they should be integrated separately with the Allam cycle. The LNG stream to be burned in the Allam cycle is integrated with the captured flue gas stream in one optimal flowsheet among Processes B-G. The major LNG stream to be directed to the natural gas pipeline is integrated with the recycled flue gas since both the flowrate of the recycled flue gas and the LNG throughput are sizeable and can be matched. The recycled flue gas consumes a huge amount of compression work (103.95 MW as shown in Table 1) before being recycled to the combustor in the Allam cycle. The LNG cold energy is abundant and can be utilized to integrate with the recycled flue gas. Similar to the standalone power plant, a direct integration process and an indirect integration process using an ORC are proposed for the cogeneration system.

Process H

The flowsheet of the cogeneration system with direct integration is illustrated in Fig.11, where LNG is integrated with the captured flue gas and recycled flue gas simultaneously. The recycled flue gas flow rate is 4,704 t/h, which is almost 30 times the captured flue gas flowrate as shown in Table 1. Based on a preliminary simulation, the LNG cold energy is not enough to liquify the recycled flue gas totally. Therefore, a separator is required to separate the liquid and gaseous flue gas after the direct integration between LNG regasification and the recycled flue gas liquefaction. The gaseous recycled flue gas is compressed to 86 bar first and then pumped to 305 bar before being fed back to the combustor. The regasified natural gas is directed to the natural gas pipeline at 30 bar.

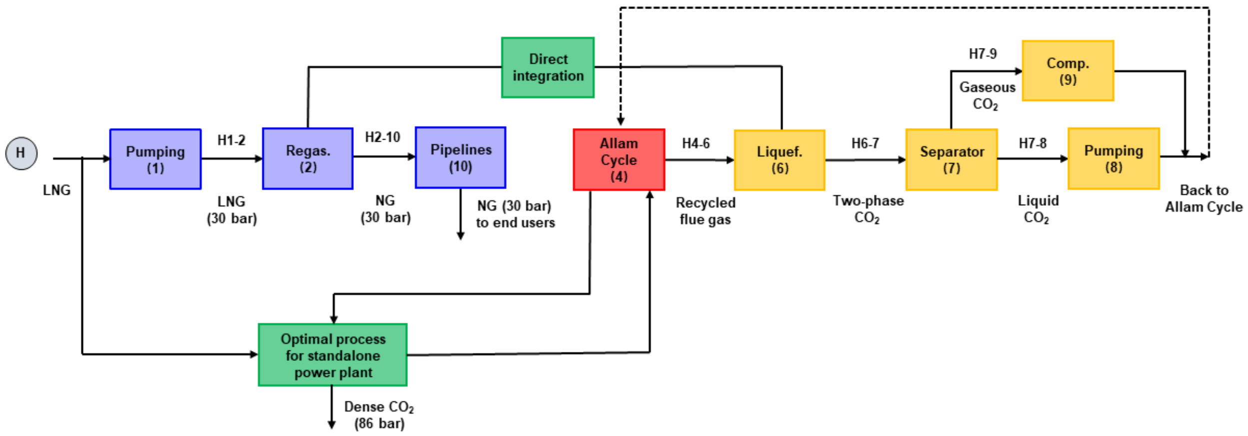

Fig.11 Flowsheet of Process H

Process I

Based on Process H, an ORC is adopted to integrate LNG regasification and recycled flue gas liquefaction in Process I as illustrated in Fig.12. Since the ORC absorbs heat from the recycled flue gas and releases the condensation heat to the LNG, the required LNG cold energy to totally liquefy the recycled flue gas stream is decreased compared with Process H. The specific amount depends on the efficiency of the ORC. The LNG can probably completely liquefy the recycled flue gas when the ORC is introduced as a bridge between LNG regasification and recycled flue gas liquefaction. Therefore, the separator in Process I can be avoided if the recycled flue gas can be completely liquified.

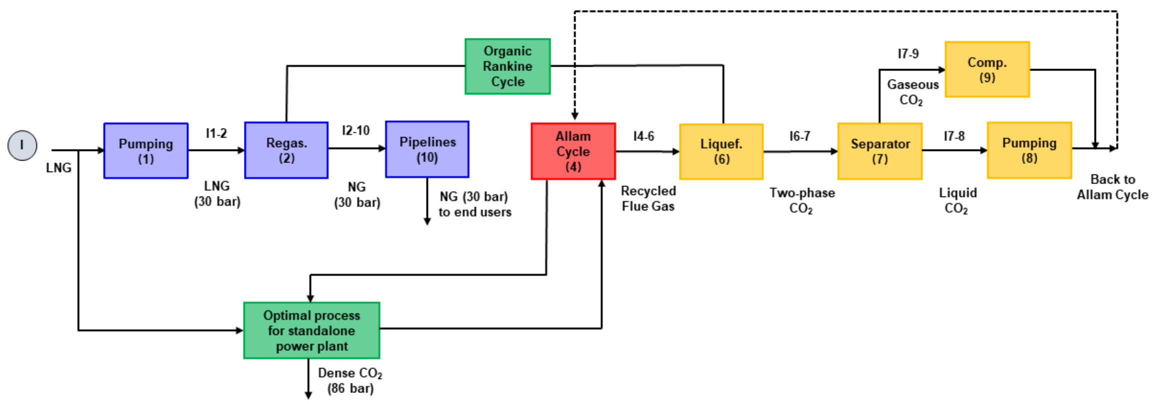

Fig.12 Flowsheet of Process I

4. Process simulation and optimization

To assess the performance of the proposed flowsheets, process simulation was carried out by Aspen HYSYS V9 [30]. The thermodynamic properties and phase behavior of the material streams in the system were calculated by a modified Peng-Robinson equation of state [31]. In addition, Aspen HYSYS [30] has the advantage of being able to simulate equipment with zero load, which facilitates the superstructure-based optimization problem. The optimal configuration can be automatically determined by an optimization algorithm. Ethane is chosen as the working fluid in this study due to the favorable critical properties of ethane in the very low-temperature range of LNG [25]. The assumptions on equipment efficiency, pressure drop, etc. are listed in Table 2. The optimal system configuration can be derived with the help of the optimization algorithm. However, the number of independent variables varies in different systems. For Process A, B and C, there are no free variables if all the heat exchangers are designed with the minimum approach temperature. Therefore, the optimization degenerates into simulation for Process A, B and C. For other Processes, an optimization algorithm has to be implemented to derive the optimal operating conditions of the system. A stochastic algorithm, Particle Swarm Optimization (PSO) [32] is adopted in this study. PSO is a population-based stochastic optimization algorithm, which is inspired by the social behavior of bird flocking [33]. Since PSO is a meta-heuristic algorithm, global optimum solutions cannot be guaranteed. The PSO algorithm in MATLAB generates random individuals, which are sent to Aspen HYSYS through an ActiveX server. The simulation outcome is retrieved from Aspen HYSYS and sent back to the optimizer in MATLAB. The simulation and optimization are performed in Aspen HYSYS and MATLAB in an alternating and iterative way until a stopping criterion is met.

Table 2. Simulation and optimization assumptions adopted in this study

Simulation Assumptions	Value	Unit
Adiabatic efficiency of compressors	0.75	-
Adiabatic efficiency of pumps	0.75	-
Pressure drop in heat exchangers	0	bar
Minimum heat exchanger temperature approach	3	K
Maximum turbine outlet liquid fraction	0.1	-
Optimization Assumptions		
Population size	50	-
Maximum generations	100	-
Maximum stall iteration	50	-
Function tolerance	1e-5	-

The objective function for the standalone LNG power plant is to minimize the total power consumption of the LNG regasification and carbon capture process as shown in Eq. (1). The power consumed by pumps and compressors has to be deducted from the gross power output. The ORC (if any) will generate electricity, thus the power output of an ORC should be added to the objective function. For the cogeneration system, the integration of the LNG substream to be burned in the Allam cycle with the captured flue gas is one of Processes A-G. Therefore, the captured flue gas integration is not considered in the cogeneration system any more. The objective function of the cogeneration system is to maximize the saved compression work with LNG cold energy utilization as expressed in Eq. (2). The constant 103,950 in Obj2 denotes recycled flue gas compression work in the original Allam cycle. 103,950 kW compression work can be saved if the LNG regasification process is integrated with the recycled flue gas. However, liquified recycled flue gas pump work (W_{pum}^{rec}), non-condensed recycled flue gas compression work (W_{com}^{rec}), LNG pump work (W_{pump}^{LNG}) and ORC pump work (W_{pump}^{ORC}) are consumed and the ORC turbine work (W_{tur}^{ORC}) is generated when the LNG regasification is integrated with the recycled flue gas compression process. Obj2 applies to Processes H and I. Finally, the optimization models can be formulated as shown by Eq. (3). The constraints include the mass and energy balance equations, models of components, equipment specifications, etc. The simulation results and the constraints are retrieved and checked by MATLAB to see if the individual solution is located in the feasible region.

$$\mathrm{Obj1} = W_{com}^{cap} + W_{pum}^{cap} + W_{pum}^{LNG} + W_{com}^{NG} + W_{pum}^{ORC} - W_{tur}^{ORC} \tag{1}$$

$$\mathrm{Obj2} = 103{,}950 - W_{pum}^{rec} - W_{com}^{rec} - W_{pum}^{LNG} - W_{pump}^{ORC} + W_{tur}^{ORC} \tag{2}$$

$$\begin{aligned}
&\text{Minimize Obj1 or Maximize Obj2}\\
&\text{s.t. Mass and energy balances, component model in Aspen HYSYS}\\
&\quad \text{Heat exchanger minimum approach temperature } \geq 3\text{K}\\
&\quad \text{Turbine outlet stream vapor fraction} \geq 0.9\\
&\quad \text{Turbine inlet stream vapor fractoin=1}\\
&\quad \text{Pump inlet stream vapor fraction =0}\\
&\quad \text{Carbon dioxide recovery rate} \geq 0.9
\end{aligned} \tag{3}$$

5. Results and discussion

5.1 Results of the standalone power plant

A preliminary energy analysis of the flue gas condensation and LNG evaporation process has been performed, assuming that the flue gas and LNG are pure CO_2 and methane, respectively. Since one mole of LNG results in one mole of CO_2, it is insightful to plot molar heat of condensation for the flue gas and molar heat of vaporization for different pressures on the same diagram as shown in Fig.13. The condensation of CO_2 should take place above the triple point of CO_2. As shown in Fig.13, beyond 6 bar, the flue gas condensation heat decreases with the increased condensation pressure. Similarly, the evaporation heat of LNG also decreases with the increased evaporation pressure. When the LNG evaporates under low pressures (less than 10 bar), the LNG can liquefy the CO_2 completely for pressures above 25 bar. However, the LNG cold energy is not enough to liquefy the CO_2 totally when the flue gas condensation pressure is at low levels (less than 25 bar). Therefore, a high condensation pressure of flue gas and a low evaporation pressure of LNG are expected from the perspective of carbon capture. However, the natural gas has to be compressed to 305 bar in the Allam cycle. A low evaporation pressure of LNG means that more work has to be consumed to compress the regasified natural gas to the target pressure. Therefore, there is a trade-off between the CO_2 liquefaction process and the natural gas compression process. The Allam cycle requires high pressure of natural gas with a corresponding large demand for compression work. However, the flue gas pressure can be as high as 33 bar, much higher than the conventional power cycles, and this reduces energy requirements of the flue gas condensation process.

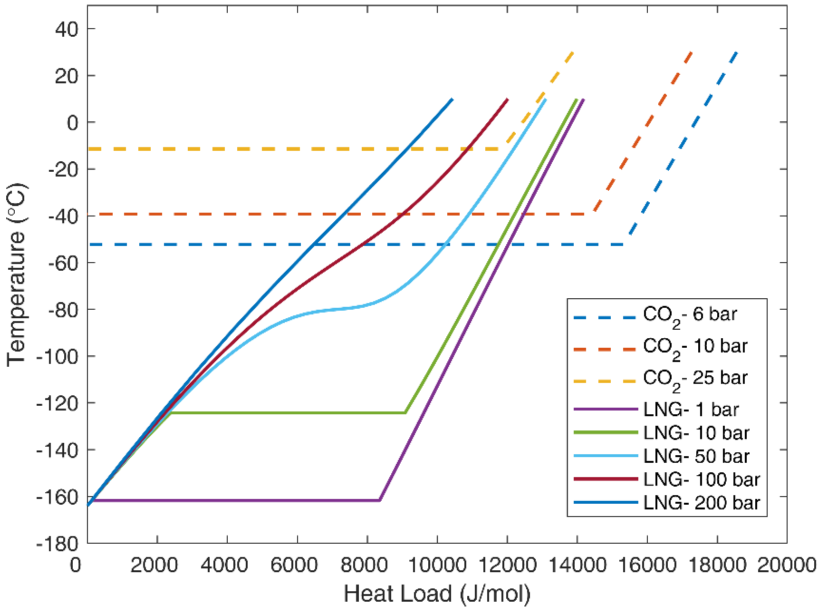

Fig.13 CO_2 condensation and LNG evaporation process under various pressures

The results for Processes A-G are summarized in Table 3. The combined contributions from the natural gas pump and compressor, the flue gas pump and compressor, and the ORC pump and turbine determine the optimal system configuration and operating conditions. The reference process (Process A) without any integration is the most inefficient system among all configurations. 2370 kW shaft work is required to compress the captured flue gas to a dense state. Energy savings can be achieved by the integration of LNG regasification and captured flue gas compression. Process B aims at utilizing the LNG cold energy to liquefy the flue gas completely (no less than 90% capture rate), and thus no flue gas compressor is needed and the flue gas compression work is replaced by pump work of 290.1 kW. In Process B, the evaporation pressure of LNG is 116.5 bar. After regasification, the natural gas is compressed to 305 bar at the cost of 2499 kW compression work. Process B eliminates the flue gas compressor but a natural gas compressor has to be configured. On the contrary, Process C aims at eliminating the natural gas compressor, which means the LNG is pumped to 305 bar directly before regasification. In Process C, the natural gas compressor is avoided but the LNG cold energy released is reduced. The LNG pump consumes 1415 kW work and 68.67% of the captured flue gas is liquified by LNG, 21.33 % is compressed to dense state by a compressor, and 10% of the captured flue gas is vented since the recovery rate is set as 90%. The hot and cold composite curves for Process C are plotted in Fig.14. The temperature difference between the flue gas and the LNG in the superheated region is quite small and the final temperature of natural gas can be as high as 25.94°C as shown in the Appendix. For Process D, both the natural gas compressor and the flue gas compressor are considered in the superstructure, which incorporates both Process B and Process C. Interestingly, the optimization results are the same as that for Process C, which means that Process C is superior to Process B. In other words, we should give priority to saving natural gas compression work, while accepting captured flue gas compression work. Based on the results for Process B, when the evaporation pressure of LNG is higher than 116.5 bar, the LNG cold energy released is not enough to liquify 90% of the flue gas.

Table 3. Results summary of different standalone power plant configurations

Process	W_{com}^{NG} (kW)	W_{pum}^{LNG} (kW)	W_{com}^{cap} (kW)	W_{pum}^{cap} (kW)	W_{tur}^{ORC} (kW)	W_{pum}^{ORC} (kW)	Obj1 (kW)	E_{in} (kW)	E_{out} (kW)	Exergy efficiency
A	0	1415	2370	0	-	-	3785	28015	20440	72.96%
B	2499	537.8	0	290.1	-	-	3327	27557	20986	76.15%
C&D	0	1415	496.8	223.9	-	-	2136	26360	20569	78.03%
E	3223	393	0	290.1	1009	66.39	2963	28203	21921	77.73%
F&G	0	1415	706.6	194.4	733.8	28.79	1611	26569	21436	80.68%

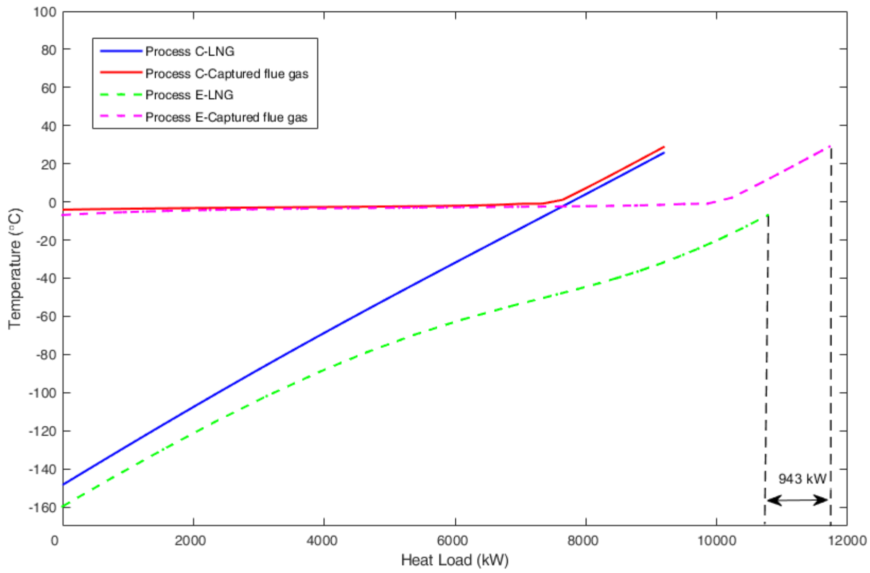

Fig.14 The composite curves for Process C(&D) and E

Processes E-G incorporate an ORC in the system to further enhance the energy efficiency of the integrated system. For the optimal configuration of Process E, the LNG is evaporated at 85.41 bar and then compressed to 305 bar consuming 3223 kW compression work. The hot and cold composite curves without considering the ORC streams are plotted in Fig.14. Since the ORC interacts with the hot and cold streams and generates electricity in the Process E, the hot and cold composite curves are not equally matched. The heat load difference (943 kW as illustrated in Fig.14) between hot and cold composite curves is exactly the net power output of the ORC. Process G incorporates both Processes E and F. Process F has fixed pressure of LNG after pumping (305 bar), while Process G treats the pressure as an optimized variable. However, the objective function values are almost the same. There is a slight difference in the ORC operating conditions for Processes F and G. Since the optimization algorithm is an evolutionary algorithm, it is normal that the results are slightly different for each run. Therefore, Process F and G can be deemed to be the same flowsheet. Processes F and G share one common set of optimal results as shown in Table 3.

Compared with the base case, the net power consumption is reduced significantly if the LNG cold energy is integrated with the carbon capture process. The net work consumption in Process

C (&D) is reduced by 43.56% ((3785-2136)/3785= 43.56%), while Process F (&G) can reduce the net power consumption by 57.43% ((3785-1611)/3785=57.43%). However, the absolute net power consumption reduction from Process C to Process F is only 525 kW.

As illustrated in Fig.14, the integration of an ORC can liquefy more flue gas in Process E compared with Process C, however, the final natural gas temperature is much lower than that in Process C, which means part of the LNG cold energy is not efficiently utilized in Process E. In addition, the LNG evaporation pressure is lower in Process E, which results in 3223 kW natural gas compression work. For Processes F (&G), even though the LNG evaporates at 305 bar, more compression work has to be consumed to compress the uncondensed flue gas. The hot and cold composite curves in Process C as shown in Fig.14 are not too far away from each other. The integration of an ORC will reduce the LNG evaporation pressure to fit in between the hot and cold composite curves. In addition, the final temperature of natural gas is much lower in Process F and G as shown in the Appendix Table, which means that part of the LNG cold energy is not fully utilized. Even though the integration of an ORC can generate extra electricity, the compensation for the natural gas compression (Process E) or flue gas compression (Process F and G) reduces the value of the ORC system.

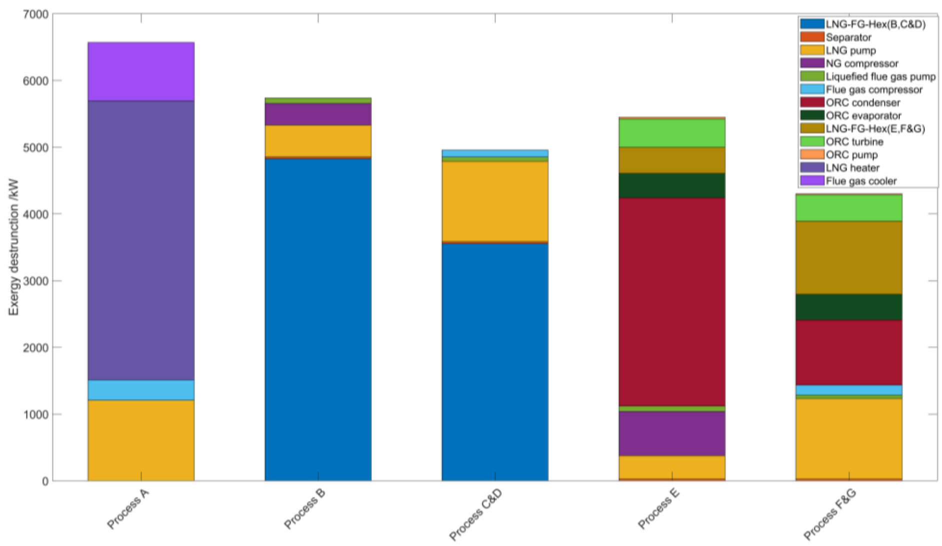

Fig.15 The exergy destruction of each process for standalone power plant

Exergy analysis is also performed for each process. The exergy input and exergy output are calculated based on the stream property in Aspen HYSYS V9. The vented stream exergy is discarded in the exergy analysis. The exergy input includes the LNG exergy, flue gas exergy, work consumed by pumps and compressors, while the exergy outputs include the natural gas exergy, captured flue gas exergy, and power output of the ORC. The exergy efficiency is defined as the ratio of exergy output to the exergy input as shown in Table 3. The exergy destruction of each equipment is also calculated and the total exergy destruction of each process is presented in Fig.15. Process E has higher exergy destruction compared with Process C (&D). Therefore, unoptimized integration of an ORC can cause more exergy destruction. Process F(&G) has the lowest exergy destruction, but the improvement is not significant relative to Process C(&D). The exergy efficiency of the reference case (Process A) is 72.96%, and Process C can improve the exergy efficiency to 78.03%. The exergy efficiency of Process C is improved by 6.95% compared with Process A. With the integration of an ORC, Process F (&G) can reach 80.68 % in exergy efficiency. Even though, the exergy efficiency of Process F (&G) is higher, the exergy efficiency is only improved by 3.4% from Process C (&D) to Process F (&G). The benefit in net power consumption is 525 kW, which may not justify the capital cost of an ORC system.

As a consequence of the high pressure of exhaust flue gas in the Allam cycle (33 bar), the power consumption for carbon capture from the flue gas is only 2370 kW (Process A). Even if the captured flue gas is completely liquified, the maximum energy saving potential is only 2079.9 kW (2370 kW-290.1 kW). However, if the flue gas pressure had been at a similar level as in a conventional combined cycle, the required compression work for the captured flue gas would increase significantly and a higher energy saving potential can be expected. In conventional combined cycle power plants, the ORC integration scheme is expected to perform much better than the direct integration scheme. In Allam cycle based power plants, the advantage of an ORC cannot be fully exploited and the performance improvement with the help of an ORC is quite limited. Process C (&D) has improved the system performance significant, but still has simple system configuration. Process C (&D) is more advantageous in terms of capital cost and system operation. Therefore, Process C (&D) is the best choice among all the proposed flowsheets for the standalone power plant.

5.2 Results of the cogeneration system

For the cogeneration system, the recycled flue gas is integrated with the large flowrate LNG stream. The recycled flue gas compression work can be saved if the LNG regasification process is integrated with the recycled flue gas pressurization process. In the Allam Cycle, the recycled flue gas compression work is 103,950 kW, which is shown in Table 1 and presented in Obj2. The compression work can be totally saved, but extra pump work, compression work (if flue gas cannot be liquified totally by the LNG) have to been consumed in the system. The optimal results are listed in Table 4. As discussed earlier, Process C (&D) is superior to the other configurations for the standalone power plant. Therefore, Process C (&D) is chosen as the flowsheet for integrating LNG and captured flue gas in the cogeneration system. The LNG regasification and the recycled flue gas liquefaction are integrated directly without considering an ORC in Process H. The results indicate that 94.45 % (refer to Appendix) of the recycled flue gas can be liquified. The remaining 5.55% of the recycled flue gas has to be compressed to dense state at the cost of 4112 kW compression work. The minimum approach temperature of a heat exchanger between the LNG and the recycled flue gas occurs in the hot end, and the LMTD is as high as 40°C. This indicates the significant exergy losses in the direct integration scheme. In Process H, the objective function value is 86,955 kW. With the LNG cold energy utilization, only 13,317 kW (4112 kW+9205 kW) compression work is required compared to 103,950 kW reported in the original study. To further increase the LNG cold energy utilization, Process I adopts an ORC to indirectly integrate the recycled flue gas and the large throughput of LNG. The ORC has two positive effects on the system efficiency. It can not only convert part of the recycled flue gas condensation heat into electricity but also reduce the compression work of the recycled flue gas. As shown in Table 4, the recycled flue gas compression work is reduced from 4112 kW to 2214 kW, which means Process I can liquify more recycled flue gas. 96.94% of the recycled flue gas can be liquified in Process I, while the liquefaction fraction is 94.45% in Process H. This is also the reason why the recycled flue gas pumping work is increased from 9205 kW to 9406 kW. It is worth noting that the ORC system can generate 50,435 kW electricity, which is almost 9.5% of the gross power output of the Allam cycle. The thermal efficiency of the ORC in Process I is about 15%. The exergy input and output of Processes H and I is calculated as well. The exergy efficiency of Processes H and I are 71.05% and 78.48% respectively. The exergy efficiency of the system is improved by 10.45% with the integration of an ORC. For the cogeneration system, the configuration with ORC can reduce the exergy losses and improve the net power output of the system substantially.

Table 4. Results summary of different cogeneration system configurations

Process	W_{pum}^{LNG} (kW)	W_{com}^{rec} (kW)	W_{pum}^{rec} (kW)	W_{tur}^{ORC} (kW)	W_{pum}^{ORC} (kW)	Obj2 (kW)	E_{in} (kW)	E_{out} (kW)	Exergy efficiency
H	3678	4112	9205	-	-	86,955	703,573	499,907	71.05%
I	3678	2214	9406	50,435	2544	136,561	704,421	552,850	78.48%

Several findings can be derived based on the optimal results of the different system configurations studied here. For the standalone LNG power plant, the LNG cold energy should be integrated with the flue gas directly. An ORC can only improve the exergy efficiency of the system by 3.4% compared with the direct integration without an ORC. Therefore, the direct integration scheme (Process C&D) is a more favorable flowsheet for the standalone power plant. For the cogeneration system, the indirect integration of an ORC system can improve the net power output of the system substantially. The ORC has two-fold benefits on the cogeneration system. First, it can generate 50,435 kW of electricity, which is almost 9.5% of the gross Allam cycle power plant. Second, the ORC can decrease the compression work for the recycled flue gas substantially. The exergy efficiency of the Process I can be as high as 78.48%, which is 10.45% higher than that of Process H. Therefore, the cogeneration system with an ORC integration is a promising technology for simultaneous power generation and LNG regasification.

6. Conclusion

This study investigates the optimal utilization of LNG cold energy in an Allam cycle power plant. A superstructure is proposed to model multiple possible processes and determine the optimal process. The LNG cold energy can be utilized to reduce the energy penalty in CCS or reduce the compression work of the recycled flue gas compression process. Direct integration and indirect integration with an ORC are simulated, optimized and compared in this work. The trade-off among LNG regasification process, carbon capture process and organic Rankine cycle system is studied based on the simulation-based optimization framework. The following conclusions can be derived in this study.

- For the standalone power cycle, the LNG cold energy is limited and can be used to liquefy the captured flue gas. The results indicate that the indirect integration scheme with an ORC can only improve the system efficiency to a small extent. The direct integration with LNG evaporating at 305 bar is a more favorable way to utilize LNG cold energy in a standalone LNG power plant. The exergy efficiency of the system is improved from 72.96% to 78.03%. The benefit of the integration of an ORC is marginal, since compared with the direct integration the exergy efficiency can be only improved by 3.4%, which may not justify the capital cost of the ORC system.
- For a cogeneration system, the large throughput LNG regasification process can be integrated with the recycled flue gas. In this case, the indirect integration with an ORC presents significant improvement compared with the direct integration. 50,435 kW electricity can be generated by the ORC. The exergy efficiency of the direct integration

and indirect integration with an ORC are 71.05% and 78.48 respectively. The exergy efficiency can be improved by 10.45% with the integration of an ORC.

- The capital cost of the system is out of scope of this study, however the constraints set in the optimization model can guarantee the capital cost is within reasonable range. Detailed techno-economic analysis will be performed in the future research.

Appendix

Table A.1 Stream data for all the processes investigated in this study

Porcess	Stream ID	Pressure (bar)	Temperature (°C)	Flowrate (kg/h)
A	A1-2	1	0	59,470
	A2-4	305	190.40	59,470
	A4-5	33	29.00	157,300
B	B1-2	116.5	-158.10	59,470
	B2-3	116.5	25.87	59,470
	B3-4	305	105.00	59,470
	B4-6	33	29.00	157,300
	B6-8	86	-1.65	141,896
C&D	C1-2	305	-148.40	59,470
	C2-4	305	25.94	59,470
	C4-6	33	29.00	157,300
	C6-7	33	-4.09	157,300
	C7-8	33	-4.09	108,355
	C7-9	33	-4.09	33,170
E	E1-2	85.41	-159.7	59,470
	E2-3	85.41	-7.01	59,470
	E3-4	305	97.88	59,470
	E4-6	33	29.00	157,300
	E6-8	33	-6.87	141,896
	$S_{pum,inlet}^{ORC}$	5.48	-50.23	58,459
	$S_{pum,outlet}^{ORC}$	20.61	-48.91	58,459
	$S_{tur,inlet}^{ORC}$	20.61	25.97	58,459
	$S_{tur,outlet}^{ORC}$	5.48	-30.06	58,459
F&G	F1-2	305	-148.40	59,470
	F2-4	305	-5.18	59,470
	F4-6	33	29.00	157,300
	F6-7	33	-3.59	157,300

	F7-8	33	-3.59	93,968
	F7-9	33	-3.59	47,557
	$S^{ORC}_{pum,inlet}$	1	-88.97	20,578
	$S^{ORC}_{pum,outlet}$	21.62	-87.66	20,578
	$S^{ORC}_{tur,inlet}$	21.62	25.99	20,578
	$S^{ORC}_{tur,outlet}$	1	-84.66	20,578
H	H1-2	30	-162.5	1,620,000
	H2-10	30	26	1,620,000
	H4-6	33	29	4,794,000
	H6-7	33	-8.37	4,794,000
	H7-8	33	-8.37	4,528,162
	H7-9	33	-8.37	265,547
I	I1-2	30	-162.5	1,620,000
	I2-10	30	-8.00	1,620,000
	I4-6	33	29	4,794,000
	I6-7	33	-9.86	4,794,000
	I7-8	33	-9.86	4,652,829
	I7-9	33	-9.86	140,880
	$S^{ORC}_{pum,inlet}$	2.74	-67.92	2,007,785
	$S^{ORC}_{pum,outlet}$	20.48	-66.60	2,007,785
	$S^{ORC}_{tur,inlet}$	20.48	26.00	2,007,785
	$S^{ORC}_{tur,outlet}$	2.74	-52.79	2,007,785

Acknowledgments

The authors would like to acknowledge John Bradley and MIT Energy Initiative CCUS Low Carbon Energy Center for the financial support of the research.

Nomenclature

Acronyms and Abreviations	
ASU	Air separation unit
CCS	Carbon capture and storage
Comp.	Compression
GHG	Greenhouse gas
IGCC	Integrated gasification combined cycle
LAES	Liquid air energy storage
Liquef.	Liquefaction
LNG	Liquified natural gas
NG	Natural gas
ORC	Organic Rankine cycle
Regas.	Regasification

PSO	Particle swarm optimization
S	Stream
Variables	
P	Pressure
W	Work
Subscripts	
AC	Allam Cycle
cap	Captured flue gas
com	Compressor/Compression
inlet	Inlet stream of a piece of equipment
net	Net power output
outlet	Outlet stream of a piece of equipment
pum	Pump
rec	Recycled flue gas
tur	Turbine

References

[1] Blasing T, Smith K. Recent greenhouse gas concentrations. 2013.

[2] Williams JH, DeBenedictis A, Ghanadan R, Mahone A, Moore J, Morrow WR, et al. The technology path to deep greenhouse gas emissions cuts by 2050: the pivotal role of electricity. science. 2012;335(6064):53-9.

[3] Selosse S, Ricci O. Carbon capture and storage: Lessons from a storage potential and localization analysis. Applied Energy. 2017;188:32-44.

[4] Akorede M, Hizam H, Ab Kadir M, Aris I, Buba S. Mitigating the anthropogenic global warming in the electric power industry. Renewable and sustainable energy reviews. 2012;16(5):2747-61.

[5] Bui M, Adjiman CS, Bardow A, Anthony EJ, Boston A, Brown S, et al. Carbon capture and storage (CCS): the way forward. Energy & Environmental Science. 2018;11(5):1062-176.

[6] Kanniche M, Gros-Bonnivard R, Jaud P, Valle-Marcos J, Amann J-M, Bouallou C. Pre-combustion, post-combustion and oxy-combustion in thermal power plant for CO2 capture. Applied Thermal Engineering. 2010;30(1):53-62.

[7] Sipöcz N, Tobiesen A, Assadi M. Integrated modelling and simulation of a 400 MW NGCC power plant with CO2 capture. Energy Procedia. 2011;4:1941-8.

[8] Brunetti A, Scura F, Barbieri G, Drioli E. Membrane technologies for CO2 separation. Journal of Membrane Science. 2010;359(1-2):115-25.

[9] Dowling AW, Vetukuri SRR, Biegler LT. Large-scale optimization strategies for pressure swing adsorption cycle synthesis. AIChE Journal. 2012;58(12):3777-91.

[10] Tuinier M, Hamers H, van Sint Annaland M. Techno-economic evaluation of cryogenic CO2 capture—A comparison with absorption and membrane technology. International Journal of Greenhouse Gas Control. 2011;5(6):1559-65.

[11] Fu C, Gundersen T. Carbon Capture and Storage in the Power Industry: Challenges and Opportunities. Energy Procedia. 2012;16, Part C:1806-12.

[12] Yu H, Eason J, Biegler LT, Feng X, Gundersen T. Process optimization and working fluid mixture design for organic Rankine cycles (ORCs) recovering compression heat in oxy-combustion power plants. Energy Conversion and Management. 2018;175:132-41.

[13] Pan Z, Zhang L, Zhang Z, Shang L, Chen S. Thermodynamic analysis of KCS/ORC integrated power generation system with LNG cold energy exploitation and CO2 capture. Journal of Natural Gas Science and Engineering. 2017;46:188-98.

[14] Sanz W, Jericha H, Moser M, Heitmeir F. Thermodynamic and economic investigation of an improved Graz cycle power plant for CO2 capture. Journal of Engineering for Gas Turbines and Power. 2005;127(4):765-72.

[15] Scaccabarozzi R, Gatti M, Martelli E. Thermodynamic analysis and numerical optimization of the NET Power oxy-combustion cycle. Applied Energy. 2016;178:505-26.
[16] Allam R, Martin S, Forrest B, Fetvedt J, Lu X, Freed D, et al. Demonstration of the Allam Cycle: An Update on the Development Status of a High Efficiency Supercritical Carbon Dioxide Power Process Employing Full Carbon Capture. Energy Procedia. 2017;114:5948-66.
[17] Park J, Lee I, You F, Moon I. Economic Process Selection of Liquefied Natural Gas Regasification: Power Generation and Energy Storage Applications. Industrial & Engineering Chemistry Research. 2019;58(12):4946-56.
[18] Lee I, You F. Systems design and analysis of liquid air energy storage from liquefied natural gas cold energy. Applied Energy. 2019;242:168-80.
[19] Lin W, Huang M, He H, Gu A. A transcritical CO2 Rankine cycle with LNG cold energy utilization and liquefaction of CO2 in gas turbine exhaust. Journal of Energy Resources Technology. 2009;131(4):042201.
[20] Shi X, Agnew B, Che D, Gao J. Performance enhancement of conventional combined cycle power plant by inlet air cooling, inter-cooling and LNG cold energy utilization. Applied Thermal Engineering. 2010;30(14):2003-10.
[21] Xiong Y, Luo P, Hua B. A novel CO2-capturing natural gas combined cycle with LNG cold energy utilization. Energy Procedia. 2014;61:899-903.
[22] Sifat NS, Haseli Y. Thermodynamic modeling of Allam cycle. Conference Thermodynamic modeling of Allam cycle, Pittsburgh, 2018. American Society of Mechanical Engineers Digital Collection, p. 1-5.
[23] McCoy ST, Rubin ES. An engineering-economic model of pipeline transport of CO2 with application to carbon capture and storage. International Journal of Greenhouse Gas Control. 2008;2(2):219-29.
[24] IEAGHG. Oxy-combustion turbine power plants. International Energy Agency; 2015.
[25] Yu H, Kim D, Gundersen T. A study of working fluids for Organic Rankine Cycles (ORCs) operating across and below ambient temperature to utilize Liquefied Natural Gas (LNG) cold energy. Energy. 2019;167:730-9.
[26] Yu H, Feng X, Wang Y, Biegler LT, Eason J. A systematic method to customize an efficient organic Rankine cycle (ORC) to recover waste heat in refineries. Applied Energy. 2016;179:302-15.
[27] Romeo LM, Lara Y, González A. Reducing energy penalties in carbon capture with Organic Rankine Cycles. Applied Thermal Engineering. 2011;31(14):2928-35.
[28] Baldwin P, Williams J. Capturing CO2: Gas Compression vs. Liquefaction. Power Mag. 2009;113(6):68-71.
[29] Lee U, Han C. Simulation and optimization of multi-component organic Rankine cycle integrated with post-combustion capture process. Computers & Chemical Engineering. 2015;83:21-34.
[30] HYSYS A. AspenTech. Calgary; 2007.
[31] Jaubert J-N, Mutelet F. VLE predictions with the Peng–Robinson equation of state and temperature dependent kij calculated through a group contribution method. Fluid Phase Equilibria. 2004;224(2):285-304.
[32] Eberhart R, Kennedy J. A new optimizer using particle swarm theory. Conference A new optimizer using particle swarm theory. IEEE, p. 39-43.
[33] Garg P, Orosz MS. Economic optimization of Organic Rankine cycle with pure fluids and mixtures for waste heat and solar applications using particle swarm optimization method. Energy Conversion and Management. 2018;165:649-68.